Aging Characteristics and Effects of Plastic Deformation on Precipitation in Al-4% Cu and Al-20% Ag Alloys with or without Trace Elements

AUTHOR(S):

MURAKAMI, Yotaro; KAWANO, Osamu; TAMURA, Hideaki

CITATION:

MURAKAMI, Yotaro ...[et al]. Aging Characteristics and Effects of Plastic Deformation on Precipitation in Al-4% Cu and Al-20% Ag Alloys with or without Trace Elements. Memoirs of the Faculty of Engineering, Kyoto University 1964, 26(1): 34-68

ISSUE DATE:

1964-03-16

URL:

http://hdl.handle.net/2433/280587

Aging Characteristics and Effects of Plastic Deformation on Precipitation in Al-4% Cu and Al-20% Ag Alloys with or without Trace Elements

By

Yotaro MURAKAMI*, Osamu KAWANO*
and Hideaki TAMURA*

(Received October 31, 1963)

The experiments have been carried out to examine the effects of plastic deformation and addition of small amounts of third elements on the aging process in Al-4% Cu and Al-20% Ag alloys by the X-ray Laue method, microhardness measurements, transmission electron microscopic studies and resistivity measurements. In binary Al-4% Cu alloys, the plastic deformation immediately after quenching retards the growth of G.P. (1) and G.P. (2), and accelerates the nucleation of the θ' phase. In Al-20% Ag alloys, similar results are obtained. In undeformed ternary Al-Cu alloy, the retarding effects of third elements on aging become stronger in the order Be<Ti<Zr. In Al-Cu-Zr alloys, the plastic deformation much accelerates the growth of G.P. (1). The role of excess vacancies on aging and the interaction between dislocation and precipitates are discussed.

1. Introduction

Several researchers have studied the effects of plastic deformation prior to aging and the addition of small amounts of third elements on the aging process of age-hardenable binary aluminium alloys.

Since it is clear that lattice defects, such as vacancies and dislocations play an important role on formation and growth of Guinier-Preston Zones, it is very interesting to study the effects of plastic deformation immediately after quenching. It is accepted that small clusters are formed rapidly just after or during plastic deformation at room temperature[1)2)].

Recent works[3)~5)] have shown that plastic deformation by small amounts retards the growth of zones in various age-hardenable alloys. Two hypotheses have been discussed to account for the phenomenon. In one of these, it is supposed that quenched-in vacancies, which are necessary for solute diffusion,

* Department of Metallurgy

are swept out by the motion of dislocations during plastic deformation or that the rate of annealing out of vacancies is increased. This hypothesis received some support, because in the air cooled alloys suppressive effects of cold working on aging are found to be less than in ice-water quenched specimens from the measurements of electrical resistance[3]. The second hypothesis postulates from the calculation of interaction energies that the suppressive effects of plastic deformation at lower aging temperature are due to the interaction between solute atoms and lattice defects such as dislocations introduced by deformation[3]. According to Guinier[6], the number of defects in the deformed alloys is much higher than in the undeformed specimens and they rapidly attract the solute atoms situated in their vicinity, forming clusters too small to make a significant contribution to resistivity or hardening. Therefore, the development of the normal larger zones which contribute to age-hardening is retarded because the majority of the solute atoms already is in rather stable positions.

Pronounced effects of addition of small amounts of Sn, Cd or In (0.05% to 0.1%) on the aging process of Al-Cu alloys were extensively examined by A. H. Sully and others[7]. The research on the ternary alloys showed that the rate of high temperature aging tends to be accelerated and that the formation of G. P. zone at a low aging temperature may actually be hindered. Hardy[8] suggested three mechanisms for the marked suppression of G. P. zone formation by addition of Sn, Cd or In: (1) The ternary elements may reduce the quenching stresses. Here the quenching stresses are supposed to be the cause of the rapid rate of G. P. zone formation in binary Al-Cu alloys. (2) The ternary elements may be attached to dislocations to form obstacles against the pipe diffusion of copper atoms along dislocations. Here, the pipe diffusion is supposed to be the cause of the rapid rate of G. P. zone formation. (3) Because Sn atoms (as well as Cd and In atoms) are larger than Al atoms, (Table 1) they may collect Cu atoms, smaller than Al atoms, around them so as to reduce the strain energy. Hence, the number of Cu atoms available to the G. P. zone formation is reduced.

Table 1. Difference of atomic radii of solute atoms, compared with that of aluminium

Solute element	Be	Cu	Ag	Ti	Cd	In	Sn	Sb	Zr	Tl	Pb	Bi
Dif. with Al in %	−22.8	−10.5	+1.7	+2.8	+6.7	+10.2	+10.9	+11.8	+11.9	+20.0	+22.5	+27.7

Now it is almost certain that the excess vacancies quenched-in from the solution treatment temperature are responsible for the rapid rate of clustering of solute atoms or G. P. zone formation in some aluminium alloys e.g., Al-Cu,

Al–Ag and Al–Zn[9)~13)]. Moreover, transmission electron microscopy showed no correlation between dislocation and the G. P. zone formation[14)15)]. Therefore, the first two suggestions by Hardy are difficult to accept. The third suggestion may not be ruled out by the quenched-in excess vacancy mechanism, but it is hard to see, as pointed out by Hardy himslef, how it could be possible for such a small amount of Sn (in order of 0.01 at%) to collect the majority of Cu atoms of about 2 at%).

Kimura and Hashiguti[16)] suggested the mechanism for marked suppression of G. P. zone formation by addition of small amounts of Sn on Al–Cu alloys. Sn atoms are considered to attract the quenched-in excess vacancies more strongly than Cu atoms, so that the majority of excess vacancies quenched-in from a solution treatment temperature is bound to Sn atoms and cannot enhance the copper clustering. This explanation seems to be preferable than others.

The insoluble elements, Sb, Tl, Pb, and Bi have no influence on the aging of the aluminium-copper alloys[17)].

A detailed examination has therefore been undertaken on the aging characteristics in ternary Al–4% Cu alloys with the addition of small amounts of Be, Ti or Zr and in ternary Al–20% Ag alloys with additions of Zr. Compared with aluminium as shown in Table 1, Be has a very small atomic radius, and Zr has a very large one. The effects of plastic deformation immediately after water-quenching were also investigated in binary and ternary Al–4% Cu alloys and Al–20% Ag alloys with the X-ray Laue method, hardess measurements, and electron microscopic studies with thin foils. And especially in regard to low temperature aging, the changes of resistivity were measured.

2. Experimental Techniques

1. Preparation of alloys

Ternary Al–4% Cu alloys with Be, Ti and Zr respectively and ternary Al–20% Ag alloys with Zr were prepared from pure materials having 99.99% purity as well as binary Al–4% Cu, Al–20% Ag alloys, melting being carried out in graphite crucibles with a lining of magnesia under an atmosphere of inert argon gas, and appropriate precautions being taken to avoid contamination and superheating. The alloying elements were added to the molten aluminium in the form of mother alloys. The chemical analysis of the specimens is given in Table 2. The third element was added by the amount of 0.1 at% respectively. But as for Be the materials with 0.1 at% and 1 at% Be were made.

The chill-cast ingots, after surface machining, were homogenized for 2 days at a temperature near the solidus. The ingots were rolled into the sheet of

Table 2. Compositions of aluminium alloys (wt %).

Element / Alloy	Cu	Ag	Be	Ti	Zr
Al-Cu	4.05	—	—	—	—
Al-Cu-Be(I)	4.05	—	0.034	—	—
Al-Cu-Be(II)	3.91	—	0.31	—	—
Al-Cu-Ti	3.86	—	—	0.27	—
Al-Cu-Zr	3.98	—	—	—	0.41
Al-Ag	—	20.51	—	—	—
Al-Ag-Zr	—	20.09	—	—	0.43

approximately 10 mm in width and 0.7 mm in thickness for X-ray Laue method, 2 mm in thickness for hardness measurements. The specimens for electron microscopic studies were rolled into sheets of 60μ thickness. For resistivity measurements, the ingots were drawn to wire of 0.6 mm diameter. The large grain of the binary and ternary Al-4% Cu alloys with Be, Ti and Zr for Laue methods were prepared by the strain-anneal method. The solution treatment was carried out under an atmosphere of argon to prevent oxidation: for 24 hours at 520°C in binary and ternary Al-4% Cu alloys, for 24 hours at 500°C in binary and ternary Al-20% Ag alloys. The specimens were quenched into iced brine. Plastic deformation was carried out immediately after solution treatment by simple extension or cold rolling.

2. X-ray technique

The Laue method is generally recommended for a rapid survey of the aging process. In the binary and ternary Al-4% Cu alloys the large-grain specimens were examined with a $[100]_{Al}$ axis parallel to the X-ray beam. Photographs were taken for the same specimen which was once solution treated and aged repeatedly. The brass holder for the sheet large-grain specimens fitted into the goniometer head, and once a crystal was oriented it could be removed for aging treatment and then replaced in the goniometer in the required orientation. Satisfactory photographs were obtained by white Cu radiation with exposures of 30 min. at 60 mA, 35 KVP using a collimeter 5.5 cm in length and 0.5 mm bore with a specimen to film distance of 3.5 cm.

3. Hardness measurements

The micro-Vickers hardness was measured on the surface of the sheet specimens by using a "Durimet" micro-Vickers hardness tester under the load of 100 g. The hardness number was taken as the average of four generally close values.

4. Techniques for transmission electron microscopy

The structural changes produced by aging have been investigated by examining thin foils of these alloys by an electron microscope. The foils were prepared by the sheets of 60μ thickness, aged at various temperatures, were thinned by controlled electropolishing. It was suitable to polish electrolytically in Tajima's solution[18] at room temperature (70 ml orthophosphoric acid, 20 ml sulphuric acid, 8 g chromic oxide and 10 ml water); then Lenoir's solution[19] at 70°C (62 ml orthophosphoric acid, 13 ml sulphuric acid, 16 g chromic oxide and 24 ml water).

A slow controlled electropolishing was carried out at potential of 10–20 volt and a current of 0.1 ampere with a Pt cathode. After electropolishing the thin foils were immersed for about 20 mins into the cold solution[19], containing 17.5 ml orthophosphoric acid, 8 g chromic oxide and 32.5 ml water, to remove oxides on the surfaces. Small sections were cut with scissors from the thinnest parts of the specimens and mounted in a microscope specimen holder. Examination was carried out in a Shimazu Sm-D4 electron microscope operating at 75 kV.

5. Techniques for resistivity measurements.

A peace of wire of 0.6 mm diameter, about 30 cm in length, was bent and spot-welded to the pure aluminium wire of 0.45 mm diameter at each of the ends and fixed on a quartz frame. Specimens were heated in a vertical furnace with a temperature controlled within ± 3°C and quickly quenched into iced brine at -20°C. After quenching into iced brine, the specimen was fixed quickly on a specimen holder and transferred into an oil held at 50° or 70°C where the resistivity during the isothermal aging was measured. The plastic deformation was carried out immediately after quenching by simple extension. The voltage was measured precisely with a potentiometer, and the current by using a potentiometer and a standard resistance of 0.01 ohm.

3. Experimental Results

1. Aging characteristics and effects of plastic deformation on precipitation in Al-4%Cu alloys with or without trace elements.

(1) X-ray studies. In Al-4%Cu alloys the growth of G.P. (1) and (2) is hindered, though the precipitation of the more stable θ' phase is accelerated, by the plastic deformation immediately after water quenching. In isothermal aging at 70°C, the weak streaks due to G.P. (1) appear through {131} matrix points for 1 hour in unworked specimens as shown in photo 1, but cannot be observed in 4.5% elongated materials even for 22 days as in photo 2. According to the stereographic projection, these streaks correspond to the G.P. (1) formed on the

$(100)_{Al}$-matrix plane during aging. In as-quenched specimens, the central streaks at small angles, which show the existence of the zones formed during the quenching, increase in intensity and sharpness during the course of aging. In deformed alloys, these changes are found to be slower. In aging for 3 days at 110°C, the intense streaks and the intensity maxima[20] due to G.P. (1) and G.P. (2) appear in the undeformed alloys (photo 3) but only the weak streaks due to G.P. (1) are found in the 7.5% elongated materials (photo 4). In regard to aging for 2 hrs at 200°C, the intense streaks due to the G.P. (2) precipitation in the undeformed alloys are observed (photo 5). On the other hand, the 4.6% elongated specimen shows the diffuse θ' spots (photo 6).

In the air cooled Al-4%Cu alloys, the effects of plastic deformation were also examined. Comparing with as-quenched specimens, the central streaks due to G.P. zones formed during aging are much weaker in the air cooled alloys. In the specimens aged for 15 mins at 110°C, the streaks due to G.P. (1) could not be found in air cooled alloys. But with the same aging treatments, the iced-water quenched specimens show very definite streaks through the {131} matrix spots. Photos 7 and 8 show the photographs of unworked and 7.5% elongated Al-4% Cu alloys, aged for 3 days at 110°C, respectively. The former shows the intense streaks due to G.P. (1) and in the latter photograph the weak streaks are also observed. The rate of the formation of G.P. (1) and (2) in the air cooled specimens has been shown to be slower than in water quenched materials. Thus, it may be concluded that the excess vacancies by quenching are necessary for the formation and growth of G.P.(1) and G.P. (2) in Al-Cu alloys.

In air cooled alloys, it is found that the rate of formation of G.P. (1) and GP. (2) in cold worked specimens is also slower than in undeformed materials. But it must be emphasized that the suppressive effects of plastic deformation are not so remarkable in air cooled alloys as in water quenched specimens. In other words, the rate of decomposition in unworked alloys is more rapid in water quenched specimens than in air cooled materials. But there is no difference in the rate of decomposition for deformed alloys between water quenched and air cooled specimens.

In the reverted Al-4% Cu alloys, the effects of plastic deformation were also studied. The specimens were aged for 15 min at 110°C., then heated for 4 mins at 200°C. The pattern of the reverted specimens is just like that of the air cooled specimens from 520°C. After aging for 1 day at 110°C, the very weak streaks due to G.P. (1) are shown in the unworked specimens, but in 5.0% elongated materials the streaks are not observed. Comparing the photographs in water quenched or air cooled specimens with those in reverted ones, it may

be supposed that, as the amount of the excess vacancies is very small, the rate of the formation of G.P. (1) is very slow in the latter. On the effects of plastic deformation, it must be concluded that there are suppressive effects of working in reverted alloys, although not so remarkable as in water quenched specimens.

The effects of cold working after aging at low temperature on the further aging were investigated in Al–4% Cu alloys by the Laue method. The specimen which was aged for 30 mins at 110°C after water quenching shows the streaks due to G.P. (1). When the aged specimen was deformed by 7.5% elongation the streaks were observed to become diffuse and the central streaks were observed to be unchanged. In isothermal aging at 110°C, the pattern of worked specimen shows the slower rate of formation of G.P. (1), as compared with that of the unworked crystals. The rate of formation of G.P. (2) in deformed crystals is slower than in unworked materials. Thus, there are some suppressive effects of cold working after aging at lower temperature.

From the results of the Laue photographs in binary Al–4% Cu alloys, the relation between treatments before plastic deformation and aging time necessary for detection of G.P. (1) or G.P. (2) in the isothermal aging at 110°C were summarized in Figure 1. It shows the following results.

(a) The rate of growth of G.P. (1) or G.P. (2) is the most rapid in water quenched specimens.

(b) The suppressive effects of cold working are the most remarkable in water quenched alloys. In these specimens the growth of G.P. (1) or G.P. (2) are strongly

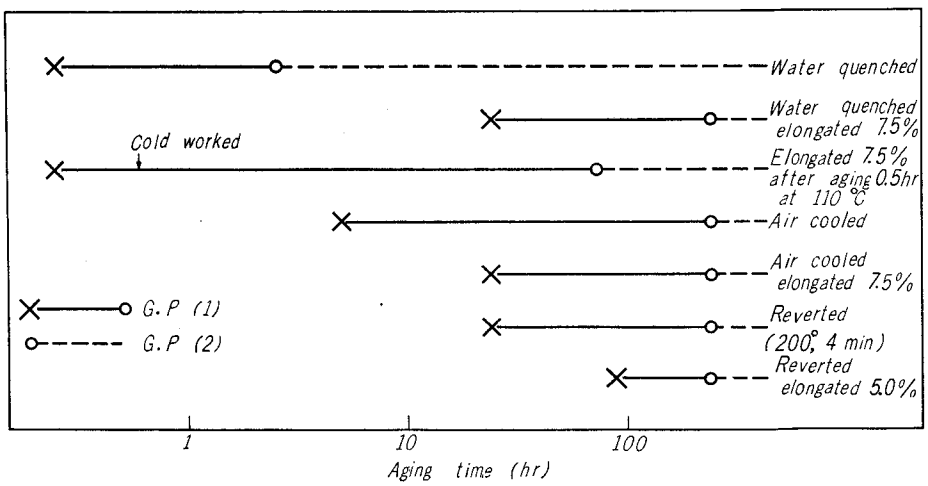

Fig. 1. Relation between treatment before cold working and aging time necessary for detection of G. P. (1) or G. P. (2) in Al–4% Cu alloys during aging at 110°C by X-ray Laue method.

retarded. In air cooled or reverted materials, such a retarding effect exists too. But the rate of formation of G.P. (2) is nearly equal in the speciments with or without cold working.

(c) The effect of cold working after aging is to retard the growth of G.P. (2).

The Laue photographs of ternary Al-4% Cu alloys with Be, Ti or Zr give the same pattern as that of the binary alloys in as-quenched specimens. This indicates that the third elements in these experiments are quite soluble into the solid solution at the tempeature of solution treatment. In isothermal aging at 100°C, the effects of plastic deformation by small amounts on aging were studied in ternary alloys with Be (0.03 and 0.3 wt%), Ti or Zr, as compared with binary alloys. The suppressive effects of cold working on the formation of G.P. (1) are clear in binary alloys as mentioned above. In Al-Cu-0.03% Be alloys, Photo 9 is the photograph of undeformed specimen aged for 3 days at 100°C. In this photograph, the G.P. (1) streaks are weaker than that in undeformed binary alloy. (Photo 3) In this alloy, the suppressive effects of plastic deformation are not observed (photo 10). In Laue photographs of Al-Cu-0.3% Be alloys, the effects of deformation were quite analogous with the alloys containing 0.03% Be. In unworked Al-Cu-Ti alloys, the rate of growth of G.P. (1) seemed to be slower than that of binary Al-Cu or Al-Cu-Be alloys. In these alloys the effects of plastic deformation on the growth of G.P. (1) and (2) are not so remarkable. In Al-Cu-Zr alloys, the {131} streaks due to G.P. (1) are not observed, after aging for 3 days at 100°C as shown in photo 11. From this result it is supposed that Zr which has a very large atomic radius as compared with Al has strong suppressive effects for the growth of G.P. (1). On the other hand, in 3.8% elongated alloys the pattern indicates that the growth of G.P. (1) is accelerated (photo 12). In comparison with photo 11, the effects of plastic deformation in Al-Cu-Zr alloys are quite different from that in binary alloys. The plastic deformation immediately after water quenching in Al-Cu-Zr alloys accelerates the formation of G.P. (1), recognized as {131} streaks in the Laue photographs. As for the isothermal aging at 100°C these appearance are summarized in Figure 2, in which representation is the same as in Figure 1. It shows the following results.

(a) The suppressive effects of G.P. (1) formation by the addition of a small amount of third elements become stronger in increasing order of magnitude Be$<$Ti$<$Zr.

(b) In Al-Cu-Zr alloys, the growth of G.P. zones is accelerated strongly by plastic deformation. But in other ternary Al-Cu alloys, the rate of G.P. (1) formation is hardly influenced by plastic deformation.

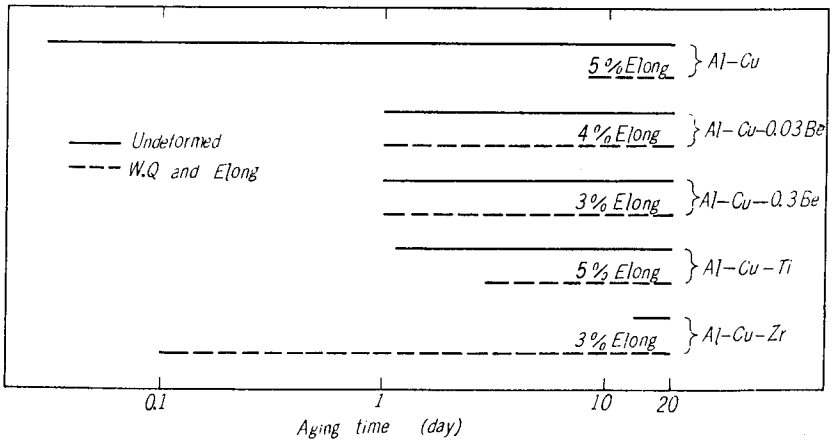

Fig. 2. Aging time required for detection G. P. (1) as streaks on X-ray Laue photographs in undeformed or deformed binary and ternary Al-4% Cu alloys during aging at 100°C.

In regard to the isothermal aging at 150°C, Laue photographs of binary Al-4% Cu alloys aged for 1 day show intense streaks and intensity maxima[20] due to G.P. (1) and G.P. (2). But for the same aging treatment only the weak G.P. (2) pattern is found in the 3.2% elongated Al-4% Cu alloys. In the Al-Cu-Ti alloys, intensity maxima due to G.P. (2) are observed weakly in unworked alloys, but in 2.0% elongated crystal G.P. (2) are detected much clearly (Photo 13 and 14). The same behaviour of cold working is found in other ternary alloys. In Al-Cu-Zr alloys, the undeformed alloy aged for 1 day at 150°C shows G.P. (2) precipitation. As compared with Al-4% Cu alloys there is no obvious difference (photo 15). But in 3.0% elongated alloys, the Al-Cu-Zr alloys show more remarkable G.P. (2) than in Al-4% Cu alloys (photo 16). Thus in the isothermal aging at 150°C, the ternary elements, especially Ti or Zr, accelerate the formation of G.P. (2), and plastic deformation accelerates the rate of G.P. (2) precipitation.

In isothermal aging at 200°C, the weak spots due to θ' appear 30 mins in undeformed Al-4% Cu alloys. In Al-Cu-Ti alloys the sharp streaks with intensity maxima due to G.P. (2) are observed for the same aging treatments. On the aging for 12 hours at 200°C, the binary and ternary Al-4% Cu alloys show more intense θ' spots, and there is no remarkable difference among them. But in ternary alloys containing Ti or Zr, G.P. (2) are thought to be more stable than Al-4% Cu or Al-Cu-Be alloys. (photos 17 and 18)

(2) Hardness measurements. Figure 3 shows the effects of cold rolling on the micro-hardness changes of Al-4% Cu alloys during aging at 70°C. In this figure, the unworked specimen shows a rapid hardening, perhaps due to G.P. (1), without

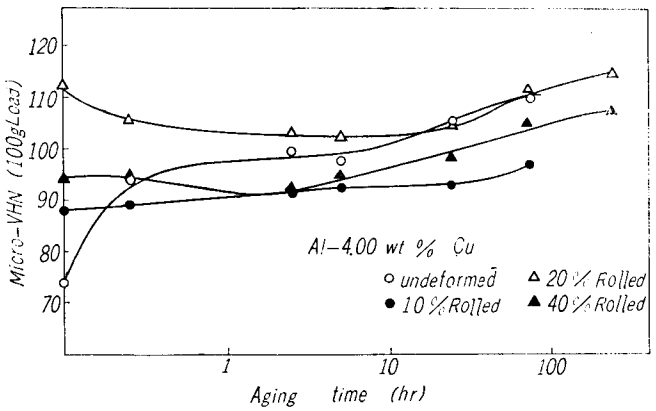

Fig. 3. Effects of cold working on microhardness changes in Al-4% Cu alloys during aging at 70°C.

incubation period. In 10% and 40% cold rolled alloys, the hardening rate is very slow. And after 1 hour at 70°C, the hardness numbers are lower than that of the unworked alloys. In 20% cold worked alloy softening during the early stage of aging is observed. And then hardness increases again just as in reversion. To examine this softening the micro-hardness was measured for the worked specimens of furnace cooled Al-4% Cu alloys under the same aging conditions. In this marked softening was not found. N. Gane and R. N. Parkins[21] made extensive studies of the hardness change in cold worked aluminium alloys during short aging treatments. Certain binary aluminium alloys exhibit rapid softening on aging for a few minutes at elevated temperatures, such as 100° or 150°C, after being cold worked at room temperature. The effect is explained in terms of the unlocking of the dislocations from the solute atmospheres that are formed during deformation.

As for the ternary Al-4% Cu alloys with Be, Ti or Zr, the micro-hardness was measured in order to verify the effects of cold working on the zone formation and precipitation.

(a) Aging at room temperature (Figure 4). The ternary alloys show a slower rate of age hardening than the binary Al-4% Cu alloys. The effect of the third elements was most remarkable in the ternary alloys containing Ti or Zr. In binary Al-4% Cu alloys, the unworked specimen shows a rapid hardening without incubation period. In 10% and 40% cold rolled alloys, the hardening rate is very slow. The deformed Al-Cu-0.03% Be alloys exhibit softening during aging. But in the other ternary alloys, 40% cold rolled materials accelerate the hardening. These results are in accordance with X-ray studies on the deformed crystals.

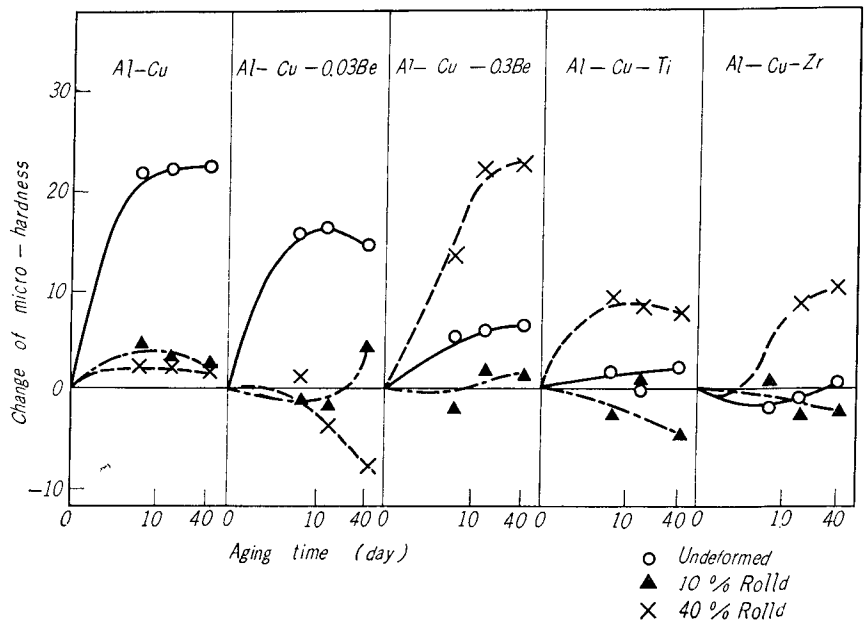

Fig. 4. Effects of cold working on microhardness changes in binary and ternary Al-4% Cu alloys during aging at room temperature.

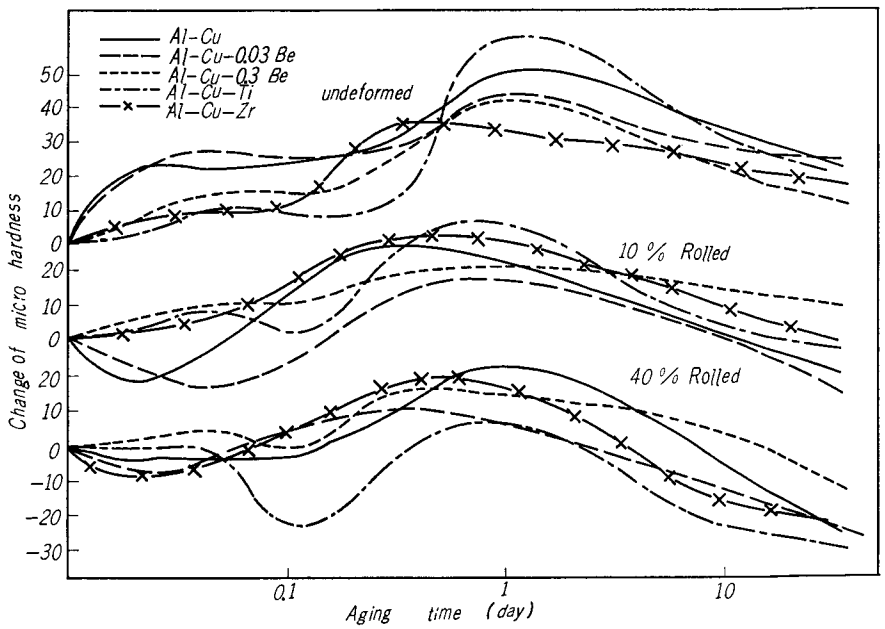

Fig. 5. Effects of cold working on microhardness changes in binary and ternary Al-4% Cu alloys during aging at 150°C.

(b) Aging at 150°C (Figure 5). The binary Al-4% Cu and Al-Cu-0.03% Be alloys give a very strong indication of a two-stage aging process at this temperature. But in the other ternary alloys this is absent from the aging curves, although the hardness increase due to G.P. (2) precipitation becomes more pronounced as shown in X-ray studies. In the 10% or 40% rolled materials, the softening is observed. In the rolled materials, the peak on the curves occured at much shorter period than in unworked alloys.

(3) Transmission electron microscopic studies. With the development of a generally applicable electropolishing thinning technique, Al-4% Cu alloys have been examined. Photo 19 shows an electron micrograph of an undeformed alloy thin foil after being aged for 2 days at 70°C. In this photograph hilical dislocations are found. It is thought that when vacancies precipitate on screw dislocation the screw component is converted to an edge dislocation by climb and as this process continues along the dislocation a helix is produced[15]. As the vacancies migrate through the lattice to form dislocation helices, they may take atoms of the solute elements with them. In 4.0% elongated specimens aged for 2 days at 70°C as shown in photo 20, the radius of the helix is smaller and the number is larger than in unworked alloys (photo 19). In both specimens, plate-like zones have not been detected. Photo 21 shows an example of G.P. (1) in Al-4% Cu alloy, aged for 20 days at 70°C. The small circular black spots about 100 Å in dia. are supposed to be G.P. (1). In this figure, dislocation loops at A and zigzag dislocations at B are found to have relationship with or without black spots due to G.P. (1). In 4.0% elongated specimens aged for 20 days at 70°C, small circular black spots are not observed and many dislocations are found in the vicinity of contour-line, e.g., at B (photo 22).

In isothermal aging for 4 days at 110°C, the small circular faint spots 200~300 Å in dia. are thought to be due to G.P. (2) in unworked materials as in photo 23. But anomalous contrast effects near the precipitates[15] could not be observed. After the same aging treatment, the 40% rolled alloys show the presence of G.P. (2) about 200 Å in dia., although in 5.0% elongated crystals the precipitates are not found (photos 24 and 25). Thus the heavy deformation such as 40% rolling seems to accelerate the growth of G.P. (1) or (2). From these results which are in good agreement with that deduced from X-ray studies, the growth of to G.P. zones is hindered by plastic deformation immediately after water quenching.

In isothermal aging at 70°C, plastic deformation by small amount retards the zone formation in Al-4% Cu alloys as mentioned above. Even after 70 days the spots due to G.P. (1) are not found in 5% elongated specimens. But in 70%

rolled binary alloys precipitates (perhaps θ') are observed in the deformed matrix. Thus it may be supposed that heavy cold working accelerates the θ' formation.

At a high temperature aging such as 160°C, the size of θ' precipitates is much larger in unworked specimen than in worked materials (photos 26 and 27). From these photographs, it is certain that plastic deformation after water quenching decreases the size of precipitates and increases the number of them. It may be supposed that the disappearance of coarse precipitates within the grains can be attributed to a large increase in the number of nucleation sites as a result of plastic deformation.

Moreover, as for isothermal aging at 200°C, photo 28 shows a micrograph of undeformed Al-4% Cu alloy, aged for 1 day at 200°C. The large θ' precipitates about 0.5μ in dia. are found in this photograph. Micrographs of θ' precipitates exhibit anomalous contrast effects near the precipitates a typical example being shown in photo 28. It is reasonalbe that the dark anomalous contrast near the precipitates in photo 28 are due to coherency strain between the precipitate and the matrix[15]. In 40% rolled alloys, aged in the same treatments, the large globular θ phase are observed along the polygon boundaries (photo 29). This phenomenon is more remarkable in the 70% rolled specimen (photo 30). In photo 30, the new recrystallized grains are observed near the grain boundary. And large black globular precipitates are found in the grain and along the grain boundary.

Further in order to study the precipitation in ternary Al-Cu alloys, thin foils of various aged alloys have been examined by transmission in the electron microscope.

Photo 31 shows an electron micrograph of an undeformed Al-Cu-Zr alloy after being aged for 70 days at 70°C. In photo 31 the irregular dislocations are observed near the grain boundaries and the zones or precipitates are not found. This photograph shows the suppression of G.P. zone formation by addition of small amounts of Zr on the aging process of Al-Cu alloys. The same results were obtained in ternary Al-4% Cu alloys containing Be or Ti. These results are similar to that deduced from X-ray studies. But in 70% cold rolled Al-Cu-Zr aged for 70 days at 70°C as shown in photo 32, large number of the small circular faint spots perhaps due to G.P. (1) are observed. Thus it may be concluded that heavy cold working creates the nucleation sites for G.P. (1) and accelerates the diffusion. These effects are more remarkable in ternary Al-Cu alloys than in binary Al-Cu alloys.

In the undeformed Al-Cu-Zr alloys the precipitates have not been found after 1 day at 150°C (photo 33). But the 5.0% elongated specimens show the

θ' precipitates as shown in photo 34. Photo 35 is the electron micrograph of the 5.0% elongated Al-Cu-0.3% Be alloy aged for 1 day at 200°C. The precipitation has occured along the helical dislocation. These helical dislocations are thought to form the polygon boundaries. In undeformed Al-Cu-Ti alloy, the size of the θ' precipitaties are smaller than in corresponding binary Al-Cu alloys (photo 36). Since the similar results were obtained in Al-Cu-Zr alloys, it may be concluded that the third elements decrease the size of precipitates. The 40% rolled Al-Cu-Ti alloys show much more smaller precipitates, perhaps θ' phase are observed along the polygon boundaries. In undeformed Al-Cu-Zr alloys, the θ' precipitates have the smallest size among the binary and ternary alloys (photo 38). In the deformed Al-Cu-Zr alloys, the size of the θ' phase decreases further and large globular θ' precipitates on polygon boundaries are not found as shown in Al-Cu-Be or Al-Cu-Ti alloys. It is certain that recrystallization of matrix may be retarded by the addition of Zr. So that, the phenomenon of the over-aging may be not remarkable in the alloy containing Zr.

(4) Resistometric investigation. Pre-precipitation phenomena of binary Al-4% Cu alloys and ternary Al-4% Cu alloys with Be, Ti or Zr were examined by means of resistivity measurements for isothermal aging at 50° or 70°C immediately after quenching from 520°C.

In Al-Cu alloys after rapid quenching from a solution treatment temperature, a marked increase in resistivity is observed within a few minutes at 0°C. The rate of change in resistivity is initially greatest and decreases with aging time. This effect is attributed to the annealing out of quenching vacancies and the formation of clustering of solute atoms[9)~13)]. The clusters formed in this stage of aging are not visible by transmission electron microscope because of their small size[14)15)]. Growth of G.P. zones follows the initial clustering, but usually needs much longer time and somewhat higher temperature. The increase in resistivity observed during low temperature aging may be due to the formation of G.P. zones. Moreover, for an alloy quenched from a high temperature, the rate of zone formation depends on the diffusion rate of solute atoms which is proportional to the excess concentration of vacancies and the mobility of vacancy-solute pairs on the aging temperature. Therefore, it is interesting to study the behavior of G.P. zone formation accompanied by plastic deformation before aging and addition of the third elements and to discuss the role of dislocation and vacancies on clustering.

Figs 6 and 7 show the changes in resistivity of binary or ternary Al-4% Cu alloys during aging at 50° or 70°C after quenching from 520°C. The longitudinal line is represented by the percentage of the increase in specific resistivity

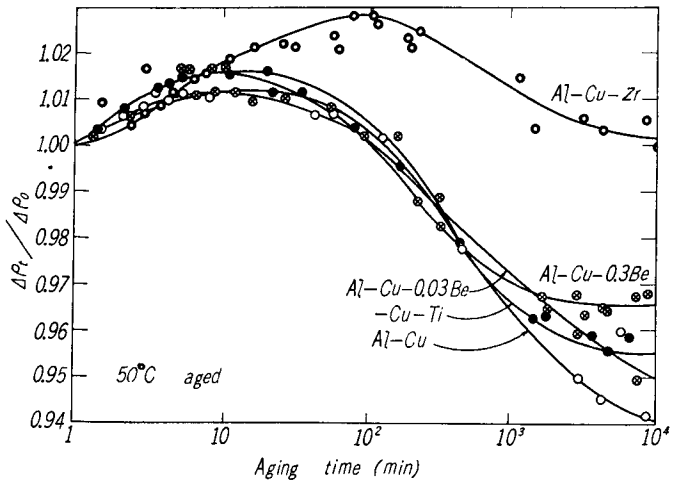

Fig. 6. Isothermal aging curves of resistivity at 50°C in binary and ternary Al-4% Cu alloys.

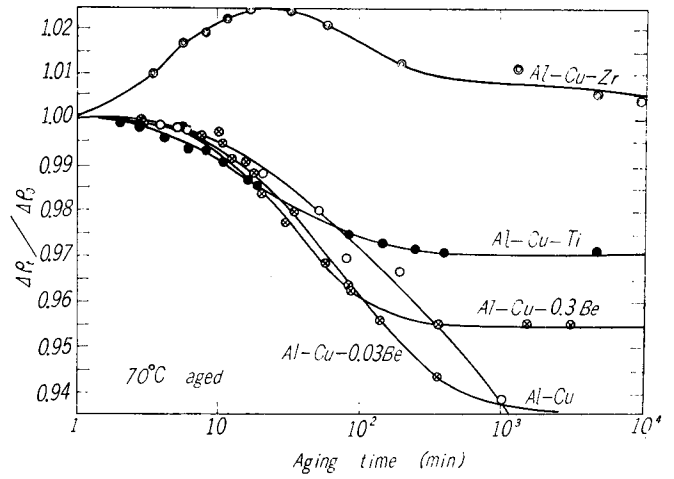

Fig. 7. Isothermal aging curves of resistivity at 70°C in binary and ternary Al-4% Cu alloys.

$\Delta\rho_t/\Delta\rho_0$. In Fig. 6, an increase in resistivity of binary and ternary Al-4% Cu alloys is observed within a few ten minutes at 50°C. Especially in Al-Cu-Zr alloys, a marked increase in resistivity is observed. This increase may be attributed to the formation of G.P. zones. Moreover in isothermal aging at 70°C in binary and other ternary aluminium alloys except Al-Cu-Zr alloys, the increases in resistivity are not found and the value in resistivity decreases with aging time as shown in Fig. 7. This fact suggests that the rate of G.P. zone formation of the ternary Al-4% Cu alloys, especially the ternary alloy containing

Zr is much slower than that in the binary Al-4% Cu alloys.

From these resistivity measurements, it is possible to explain the suppression of G.P. zone formation by addition of the third elements with the quenched-in excess vacancy mechanism. The third elements are considered to attract vacancies more strongly than Cu atoms so that the majority of excess vacancies quenched-in from a solution treatment temperature is bound to the third elements and cannot enhance the Cu clustering. The suppressive effect of G.P. zone formation is most remarkable in the ternary Al-4% Cu alloys containing Zr.

Further, the effects of plastic deformation by small amounts on the G.P. zone formation were studied in Al-4% Cu alloys with or without Zr with the resistivity measurements.

Isothermal aging curves of resistivity at 50° or 70°C after water quenching and plastic deformation are shown in Figs 8 and 9. As shown in Fig. 8 in undeformed Al-4% Cu or Al-Cu-Zr alloys a marked increase in resistivity due to the growth of G.P. (1) is observed. But in deformed Al-4% Cu alloys an increase in resistivity is not found and the rate of decrease in resistivity is slower than that in undeformed alloys. This fact suggests that since dislocations produced by plastic deformation are the sinks of excess vacancies, the increase in dislocation density by the plastic deformation lead to the rapid elimination of excess vacancies and cannot enhance the growth of G.P. (1). In deformed Al-Cu-Zr alloys, an increase in resistivity is not also observed and the behaviour of change in resistivity is similar to deformed Al-4% Cu alloys. It seems to be reasonable that the size of G.P. (1) formed on aging is fined away by plastic deformation

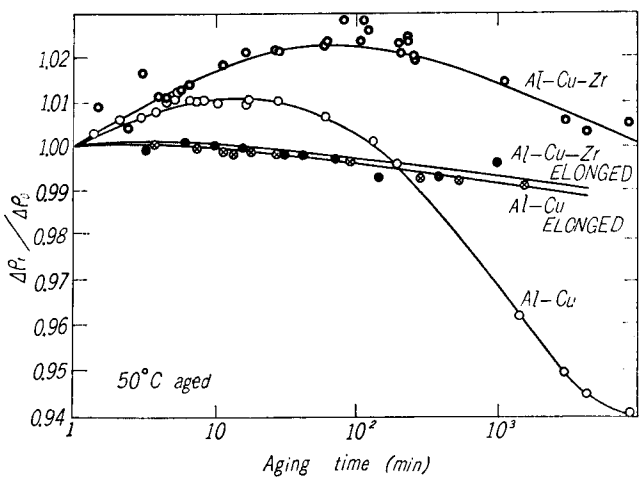

Fig. 8. Effects of cold working on resistivity changes in Al-4% Cu and Al-Cu-Zr alloys during aging at 50°C.

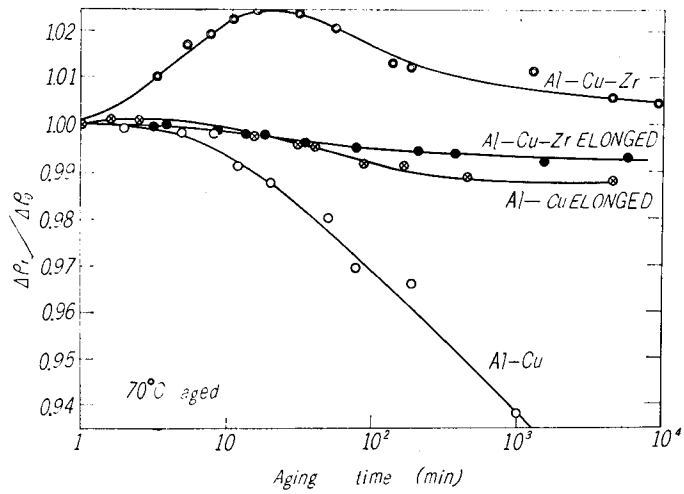

Fig. 9. Effects of cold working on resistivity changes in Al-4% Cu and Al-Cu-Zr alloys during aging at 70°C.

and the retarding effects on G.P. (1) formation by addition of Zr is weakened by plastic deformation. In Fig. 9, an increase in resistivity due to the growth of G.P. (1) is not observed in undeformed Al-4% Cu alloys but the same results are obtained as in Fig. 8. From these resistivity measurements, it may be concluded that in Al-4% Cu alloys the formation of G.P. zones is hindered by plastic deformation immediately after water quenching and that in deformed Al-Cu-Zr alloys the formation of G.P. zones is thought to be accelerated in consideration of the result of X-ray studies (Fig. 2) and hardness measurements (Fig. 4).

2. Aging characteristics and effects of plastic deformation on precipitation in Al-20%Ag alloys with or without a trace element.

Hardy and Heal[22] have suggested that the most probable sequence of precipitation in Al-Ag alloys is spherical G.P. zones→γ' plate→γ. Most Al-Ag alloys aged in the temperature range 100°~200°C have hardness-time curves which exhibit clear double peaks and Köster and Braumann[23] and Belbeoch and Guinier[24] have shown that the two peaks are associated with the successive precipitation of G.P. zones and γ'. The strengthening effect of the G.P. zones cannot be due to internal strains since the solution of Ag has very little effect on the lattice parameter of Al. The most likely explanation of the hardening has been put forward by Kelly[25] who suggested that the passage of a dislocation through an Ag-rich zone would increase the number of Al-Ag bonds, thus increasing the energy of the zone. Kelly found that the flow stress calculated

from this model was in good agreement with observed values. The high strength of alloys containing γ' has not been studied so thoroughly but Nicholson and Nutting[26] have suggested that no elastic strain field has been found in Al-16% Ag alloys at any stage of aging and the strength of the alloy is largely due to chemical hardening.

In the present investigation, the structural changes produced by aging and the effects of plastic deformation on precipitation in Al-20% Ag alloys with or without Zr have been studied by the thin foil transmission electron microscope technique and the resistivity measurements.

(1) Transmission electron microscopic studies. Guinier[27]~[29] has detected small spherical silver-rich G.P. zones in quenched Al-Ag alloys. The diameter of the zones was initially~16Å and increased rapidly during aging. In the present experiments the smallest zones which have been detected were 100~200Å in diameter and these were found after aging for 1 day at 70°C. Failure to detect smaller zones was probably due to the low resolving power of the electron microscope and being insufficient contrast between the zones and the matrix when the foil thickness was an order of magnitude greater than the zone diameter.

Photo 40 shows an electron micrograph of undeformed Al-20% Ag alloy thin foil after being aged for 14 days at 70°C. In this photograph, the small circular faint spots thought to be Ag-rich zones are observed within the grain and γ' precipitates are formed along the grain boundary and the precipitates-free region along the grain boundary is observed. In isothermal aging at 110°C, electron micrographs in undeformed Al-20% Ag alloy after 1 or 4 days show the large number of the small circular faint spots due to Ag-rich zones within the grain. These Ag-rich zones observed in these photographs are essentially similar to those observed by Nicholson and Nutting[26]. In deformed Al-20% Ag alloy aged for 4 days at 110°C, many γ' precipitates are observed (photo 43).

This fact suggests that the formation of γ' precipitates is accelerated by plastic deformation immediately after water quenching. As for Al-Ag-Zr alloys, photos 44, 45 and 46 are micrographs of undeformed specimens aged for 1 or 4 days at 110°C. The number of the small faint spots due to Ag-rich zones in Al-Ag-Zr alloys is smaller than that in binary Al-20% Ag alloys (photo 44). In photo 45, the γ' precipitates are nucleated on helical dislocation and G.P. zones continue to grow even during the formation of the γ' phase. The large number of the γ' precipitates is observed within the grain as shown in photo 46.

The γ' precipitate has a hexagonal close-packed lattice and forms in thin plate on (111) planes. Since the structure corresponds to a face centered cubic

lattice containing growth faults on every other {111} plane, the contrast due to these precipitates, is exactly like that observed from stacking faults and as shown by Nicholson characteristic fringes are produced only when a strong Bragg reflection is operating[26]. In the present investigation, these characteristic fringes are not observed. In 20% rolled Al–Ag–Zr alloys, after being aged for 4 days at 110°C, the large number of γ' precipitates are observed as shown in photo 47.

From these photographs, the effect of the small amount addition of the third elements on Ag-rich G.P. zone formation has not been studied so thoroughly but it may be suggested that the rate of zone formation is somewhat suppressed by addition of small amount of Zr. And in binary and ternary Al–20% Ag alloys, the formation of G.P. zone is hindered and the rate of γ' precipitates is accelerated by plastic deformation.

Nicholson et al[26] have suggested that the γ' phase only nucleated heterogeneously at stacking faults, e.g., at Frank-sessile dislocation or at dissociated helical dislocation. Photo 48 shows an early stage in the formation of the γ' precipitate at loops H. These become favorable nucleation sites since diffusion of Ag atoms to the defects will locally lower the stacking fault energy. These loops observed in photo 48 may be essentially similar to Frank-sessile loops observed by Nicholson. Photos 48 and 49 are micrographs of undeformed Al–20% Ag alloys aged for 0.5 hrs or 4 hrs at 200°C. Photo 49 shows arrays of large γ' precipitates which lie on {111} matrix plane. In 20% rolled Al–20% Ag alloys, aged for 4 hrs at 200°C, the number of γ' precipitates increases and the size of γ' precipitates decreases (photo 50). In ternary Al–Ag–Zr alloys, the size of γ' precipitates is much smaller than that in binary Al–Ag alloys (photo 51). Further in ternary Al–Ag–Zr alloy, the size of γ' precipitates is fine and the number of γ' precipitates increase by plastic deformation immediately after water quenching (photo 52).

(2) Resistometric investigation. The behavior of growth of zones in binary Al–20% Ag alloys and ternary Al–Ag–Zr alloys were studied by means of resistivity measurements for isothermal aging at 50° or 70°C after water quenching with or without plastic deformation as shown in Figs. 10 and 11. As shown in these figures, it is clear that the rate of resistivity decrease in deformed alloys is much less than in undeformed alloys, and that the rate of resistivity decrease in ternary alloys is much less than in binary alloys. A marked increase in resistivity as in Al–Cu–Zr alloys is not observed in binary and ternary Al–20% Ag alloys.

From these investigations, the growth of G.P. zones is hindered by plastic

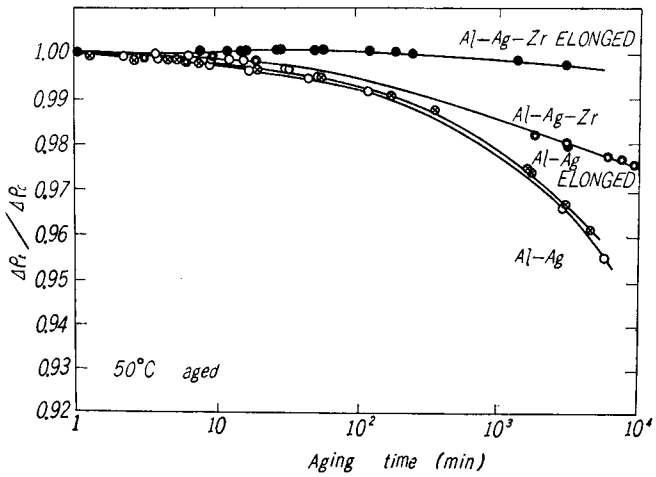

Fig. 10. Isothermal aging curves of resistivity at 50°C in undeformed or deformed binary and ternary Al-20% Ag alloys.

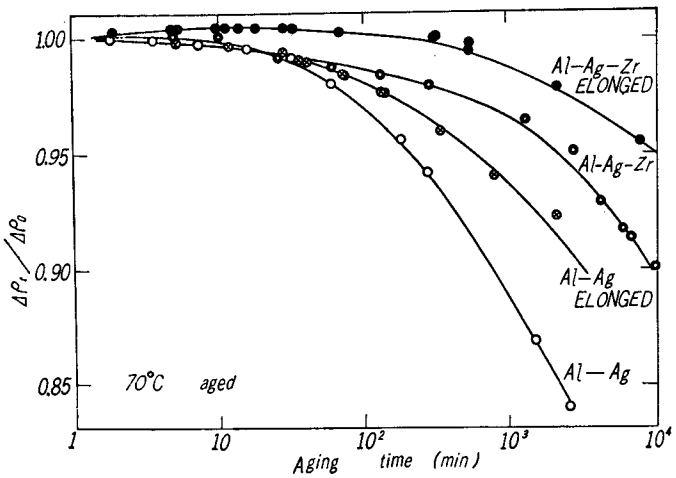

Fig. 11. Isothermal aging curves of resistivity at 70°C in undeformed or deformed binary and ternary Al-20% Ag alloys.

deformation immediately after quenching and by addition of small amounts of Zr on the aging process in Al-20% Ag alloys.

4. Discussion

On the basis of the present studies, the effects of plastic deformation after water quenching and addition of small amounts of the trace elements on precipitation of age-hardenable aluminium alloys are not simple but complex. It

seems possible that plastic deformation by small amounts actually hinders the decomposition process in the binary aluminium alloys at lower aging temperatures.

The kinetics of zone formation in Al alloys have recently been discussed by Federighi[30] and by Turnbull, Rosenbaum and Treaftis[13]. They concluded that vacancies quenched-in from solution treatment temperature are responsible for the rapid diffusion rate and low activation energies associated with the formation of zones. In the Al-4% Cu alloys, helices are observed[31][32] as shown in Photos 19 and 20. It is said that when vacancies precipitate on screw dislocation the screw component is converted to an edge dislocation by climb and as this process continues along the dislocation a helix is produced. Thus, the elimination of vacancies during the formation of these defects will allow diffusion of solute atoms to occur, and there is now little doubt that vacancies play an important role in the early stages of aging. In these experiments, the rate of the formation of G.P. (1) or G.P. (2) was slower in the air cooled or reverted Al-4% Cu alloys than in ice-water quenched materials. The suppressive effects of plastic deformation are most remarkable in ice-water quenched alloys. In air cooled or reverted crystals, such a retarding effect exists for the growth of G.P. (1). But the rate of precipitation of G.P. (2) is nearly equal in the specimens with or without cold working.

Thus the mechanism by which the rate of aging is retarded at lower aging temperature is due to the sweeping out of the quenched-in vacancies by dislocation during plastic deformation or to the increase in the rate of annealing out of quenched-in vacancies as a result of cold working[33][34].

On the other hand, it is probably generally accepted that at lower aging temperatures lattice defects, such as dislocations introduced by plastic deformation, are so stable that the solute atoms make a special distribution around the defects by the interaction between the solute atoms and lattice defects and therefore the formation of G.P. zones will be hindered. The small domains, where the concentration of solute atoms is high, have no proper well defined crystalline structure. The existence of these small clusters will be presumed from the facts that the size of precipitates is smaller in the deformed alloys than in unworked. In the above experiments, the softening observed in the aging of rolled specimens, such as reversion, seems to be due to the dissolution of smaller clusters formed during plastic deformation. But there are no evidences on the existence of these clusters by the direct observations in an electron microscope.

Retarding effects of addition of small amounts of third elements on G.P. zone formation in Al-4% Cu alloys become stronger in increasing order of

magnitude Be$<$Ti$<$Zr in the present experiments. This order may be closely related to the atomic radius of the trace elements. In ternary Al-4% Cu alloys, the interaction between excess vacancies and additional elements may be stronger than that between excess vacancies and Cu atoms, from the difference of atomic radius as shown in Table 1 and also probably from valency effects. Therefore, the majority of excess vacancies quenched-in from a solution treatment temperature is bound to the third elements and cannot enhance G.P. zone formation. And then the suppression of G.P. zone formation by addition of a small amount of Zr in Al-20% Ag alloys may be explained by the above mechanism.

In the Al-4% Cu alloys containing Zr, plastic deformation accelerates the growth of G.P. (1). Dislocations (especially edge components) produced by plastic deformation are considered to attract strongly Zr atoms, so that excess vacancies are bound to Cu atoms similarly in binary Al-4% Cu alloys and perhaps can enhance the formation of G.P. (1).

On the other hand, the acceleration of the G.P. zone formation by the plastic deformation is not observed by the resistivity measurements in ternary Al-Ag-Zr alloys. This retardation of the zone formation is considered to associate with the higher contents of Ag solute atoms. The results of electron micrographs suggest that the rate of precipitation of more stable phase is accelerated by the plastic deformation immediately after water quenching in binary and ternary Al-4% Cu alloys or Al-20% Ag alloys. The size of more stable precipitates is decreased and the number of them is increased by plastic deformation. This effect is attributed to the increase in dislocation density by the plastic deformation to provide suitable sites for nucleation of precipitates.

5. Conclusion

The effects of plastic deformation and addition of small amount of the third elements on the aging process in Al-4% Cu alloys and Al-20% Ag alloys were studied with X-ray Laue method, micro-hardness measurements, transmission electron microscopic studies and resistivity measurements.

It may be concluded that:

(1) In binary Al-4% Cu alloys, the growth of G.P. (1) and G.P. (2) is hindered by small amounts of plastic deformation. But heavy deformation accelerates the θ' precipitation. The mechanism by which the rate of formation of G.P. (1) is retarded may be explained by the next two causes: one is the sweeping out of the quenched-in vacancies by the motion of dislocations or the increase in the rate of annealing out of vacancies as a result of the increased density of dislocations and the other is the formation of many smaller clusters

of solute atoms which are formed by the stronger interaction between solute atoms and lattice defects.

(2) In ternary Al-4% Cu alloys, the suppressive effects of G.P. (1) formation by addition of small amounts of the third elements become stronger in increasing order of magnitude Be < Ti < Zr. The effects of plastic deformation in the ternary Al-4% Cu alloys are not so remarkable as in the binary alloys, but in the ternary Al-Cu-Zr alloys the plastic deformation accelerates the growth of G.P. (1).

(3) In binary Al-20% Ag alloys, the formation of spherical Ag-rich zones is hindered by plastic deformation immediately after water quenching, though the rate of precipitation of the intermediate γ' phase is much accelerated.

(4) In ternary Al-20% Ag alloys, the formation of spherical Ag-rich zones is retarded by the addition of small amounts of Zr and the growth of zones in deformed alloys is slower than in undeformed alloys.

(5) The electron micrographs indicate that the size of more stable phase is fined and the number of them is increased by plastic deformation immediately after water quenching in binary and ternary Al-4% Cu or Al-20% Ag alloys.

The present investigation was partially supported by a Research Fund provided by the Light Metal Educational Foundation, inc. of Japan for which the authors wish to express their deep appreciation. The authors express their sincere thanks to Prof. Dr. J. Takamura for discussion of results. The authors' thanks are also due to Mr. Shin-ya Komatsu who assisted in the resistivity measurements.

References

1) R. Graf and A. Guinier : Compt.rend., 238 (1954), 2175.
2) K. Matsuura, Y. Hamaguchi and S. Koda : J. Phys. Japan, 12 (1957), 1424.
3) Y. Murakami and O. Kawano : Mem. Fac. Eng. KYOTO Univ., 21 (1959), 393.
4) Y. Murakami and O. Kawano : Light Metals., 10 (1960), No. 2, 11.
5) Y. Murakami and O. Kawano : Trans. Japan Inst. Metals, 1 (1960), 27.
6) A. Guinier : J. Metals, 8 (1956), 673.
7) A. H. Sully, H. K. Hardy and T. J. Heal, J. Inst. Metals 76 (1949-50), 267.
8) H. K. Hardy, ibid 80 (1851-52), 483.
9) D. Turnbull and H. N. Treaftis, Acta Met. 5 (1957), 534.
10) W. Desorbo, H. N. Treaftis and D. Turnbull, ibid. 6 (1958), 401.
11) T. Federighi and L. Passari, ibid. 7 (1959), 422.
12) C. Panseri and T. Federighi, ibid. 8 (1960), 217.
13) D. Turnbull, H. S. Rosenbaum and H. N. Treaftis, ibid. 8 (1960), 277.
14) G. Thomas, Phil. Mag. 4 (1959), 1213.
15) R. B. Nicholson, G. Thomas and J. Nutting, J. Inst. Metals. 87 (1958-59), 429.
16) H. Kimura and R. Hashiguti, Acta Met. 9 (1961), 1076.
17) H. K. Hardy : J. Inst. Metals, 78 (1950-51), 169.

18) S. Tajima : Electropolishing and chemical polishing, 34.
19) R. B. Nicholson, G. Thomas and J. Nutting : British J. Appl. Phys, 9 (1958), 25.
20) J. M. Silcock, T. J. Heal and H. K. Hardy : J. Inst. Metals, 82 (1953-54), 239.
21) N. Gane and R. N. Parkins : ibid, 88 (1959-60), 173.
22) H. K. Hardy and T. J. Heal, Progr. Met. Phys. 5 (1954), 143.
23) W. Köster and F. Braumann, Z. Metallk. 43 (1952), 193.
24) B. Belbeoch and A. Guinier, Acta Met. 3 (1955), 370.
25) A. Kelly, Phil. Mag. 3 (1958), 1472.
26) R. B. Nicholson and J. Nutting, Acta Met. 9 (1961), 332.
27) A. Guinier, J. Phys. Radium 8 (1942), 122.
28) A. Guinier, Z. Metallk. 43 (1952), 217.
29) A. Guinier, Acta Cryst., Camb. 5 (1952), 121.
30) T. Federighi : Acta Met. 6 (1958), 379.
31) G. Thomas : Phil. Mag., 4 (1959), 606.
32) G. Thomas and M. J. Whelan : ibid, 4 (1959), 511.
33) M. Wintenbeger : Compt rend., 242 (1956), 128.
34) S. Pearson and F. J. Bradshaw : Phil. Mag., 1 (1956), 880.

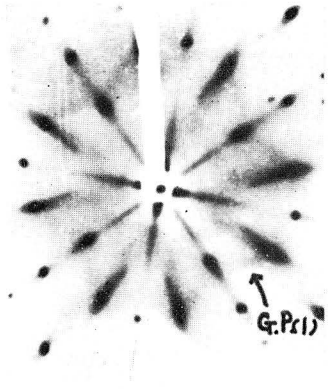

Photo. 1 Al-4% Cu alloy W.Q., aged 1 hr at 70°C.

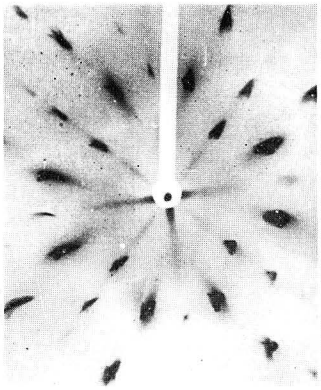

Photo. 2 Al-4% Cu alloy W.Q., elong. 4.5% and aged 22 days at 70°C.

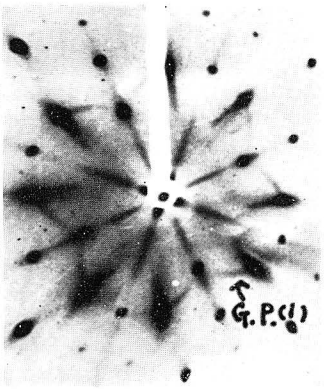

Photo. 3 Al-4% Cu alloy W.Q., aged 3 days at 110°C.

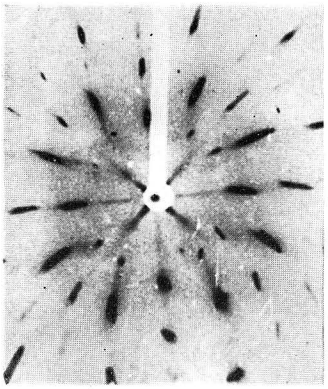

Photo. 4 Al-4% Cu alloy W.Q., elong. 7.5% and aged 3 days at 110°C.

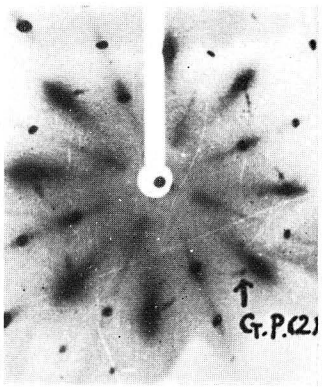

Photo. 5 Al-4% Cu alloy W.Q., aged 2 hr at 200°C.

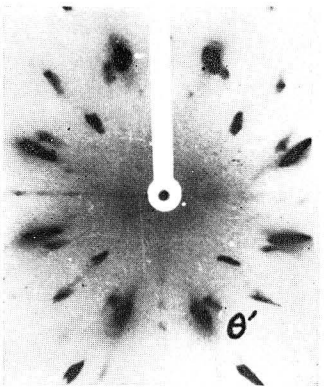

Photo. 6 Al-4% Cu alloy W.Q., elong. 4.6% and aged 2 hr at 200°C.

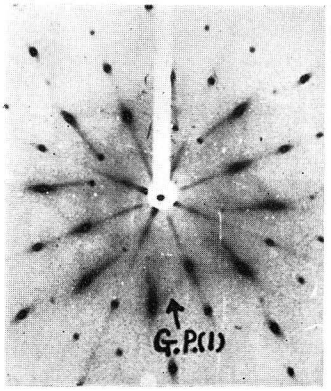

Photo. 7 Al-4% Cu alloy A.C., aged 3 days at 110°C.

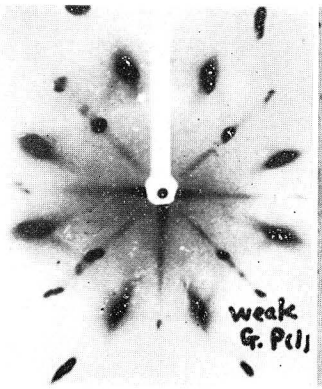

Photo. 8 Al-4% Cu alloy A.C., elong. 7.5% and aged 3 days at 110°C.

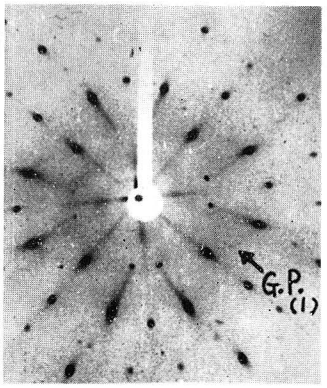

Photo. 9 Al-Cu-0.03% Be alloy, W.Q., aged 3 days at 100°C.

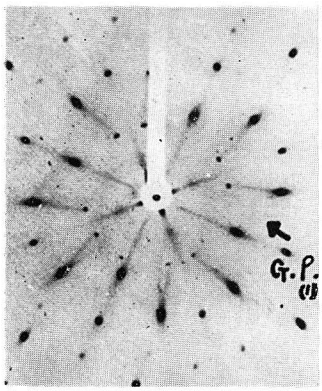

Photo. 10 Al–Cu–0.03% Be, W.Q., elong. 4.1% and aged 3 days at 100°C.

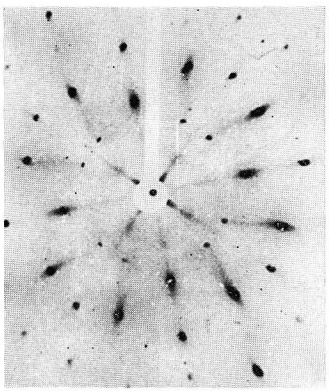

Photo. 11 Al–Cu–Zr alloy, W.Q., aged 3 days at 100°C.

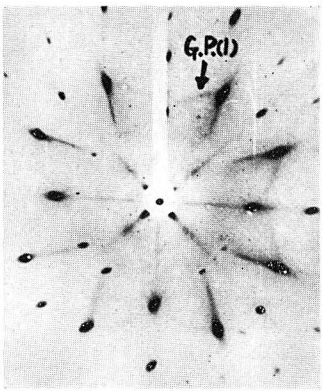

Photo. 12 Al–Cu–Zr alloy W.Q., elong. 3.8% and aged 3 days at 100°C.

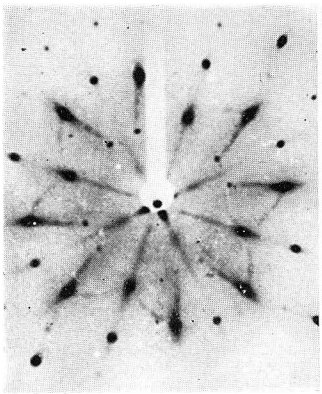

Photo. 13 Al–Cu–Ti alloy, W.Q., aged 1 day at 150°C.

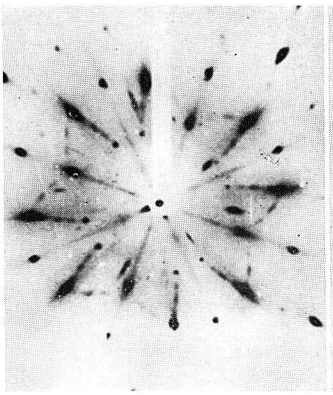

Photo. 14 Al–Cu–Ti alloy W.Q., elong. 2% and aged 1 day at 150°C.

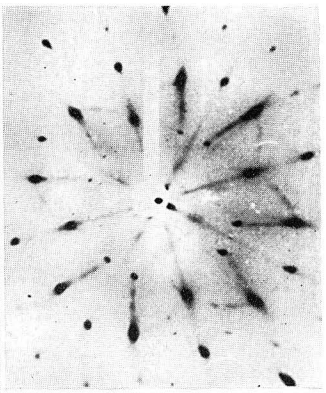

Photo. 15 Al–Cu–Zr alloy, W.Q., aged 1 day at 150°C.

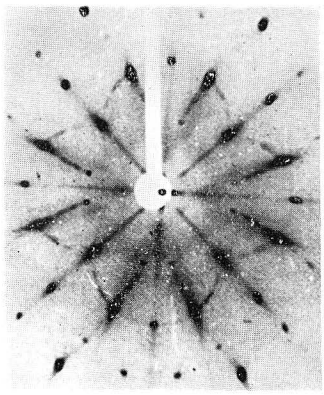

Photo. 16 Al–Cu–Zr alloy W.Q., elong. 3% and aged 1 day at 150°C.

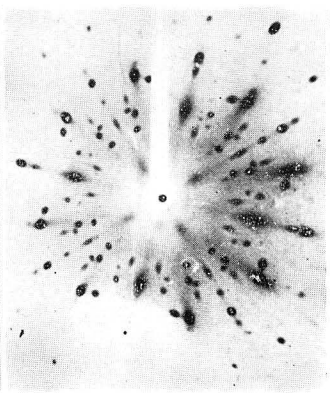

Photo. 17 Al–Cu–0.3%Be, alloy, W.Q., aged 12 hrs at 200°C.

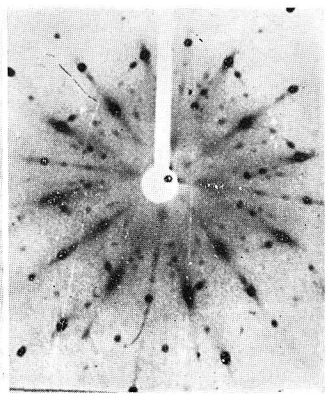

Photo. 18 Al–Cu–Zr alloy, W.Q., aged 12 hrs at 200°C.

Photo. 19 Al-4% Cu alloy, W.Q., aged for 2 days at 70°C. ×35000

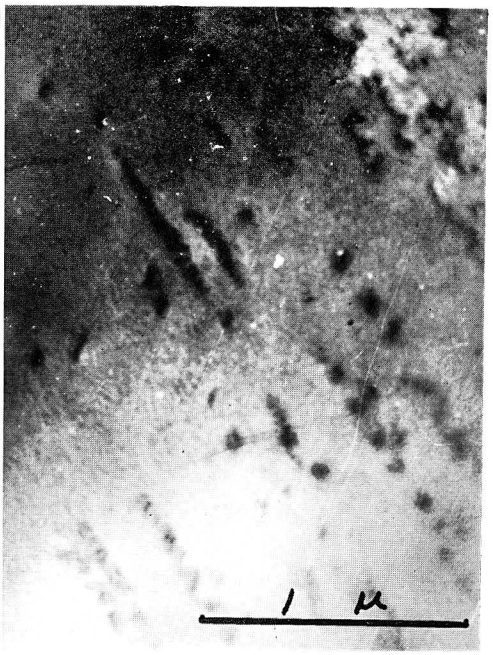

Photo. 20 Al-4% Cu alloy, W.Q., 4.0% elong., aged for 2 days at 70°C. ×35000

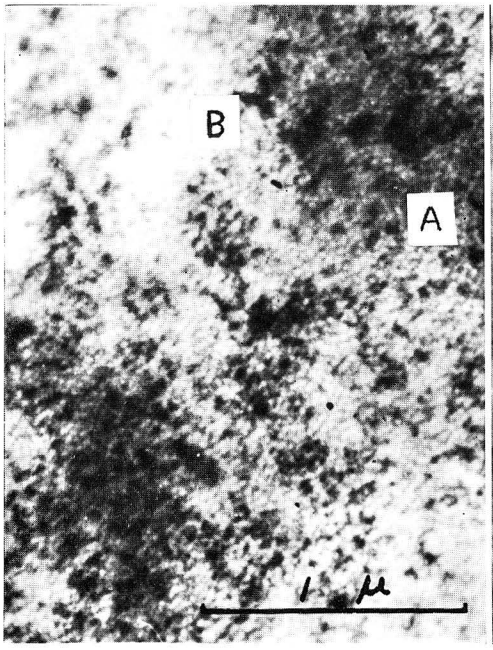

Photo. 21 Al-4% Cu alloy, W.Q., aged for 20 days at 70°C. ×35000

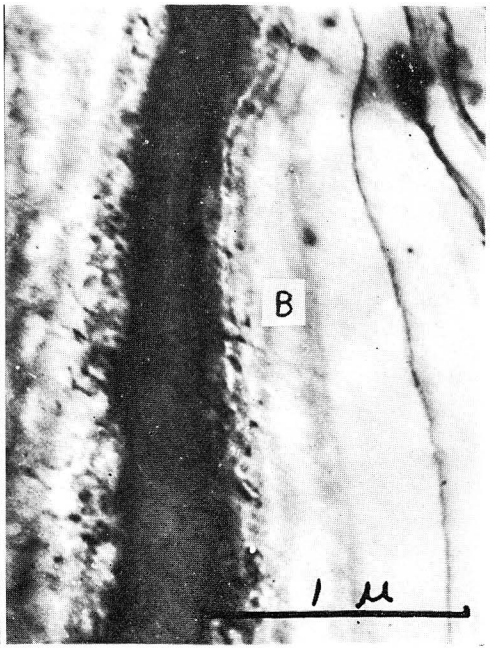

Photo. 22 Al-4% Cu alloy, W.Q., 4.0% elong., aged for 20 days at 70°C. ×35000

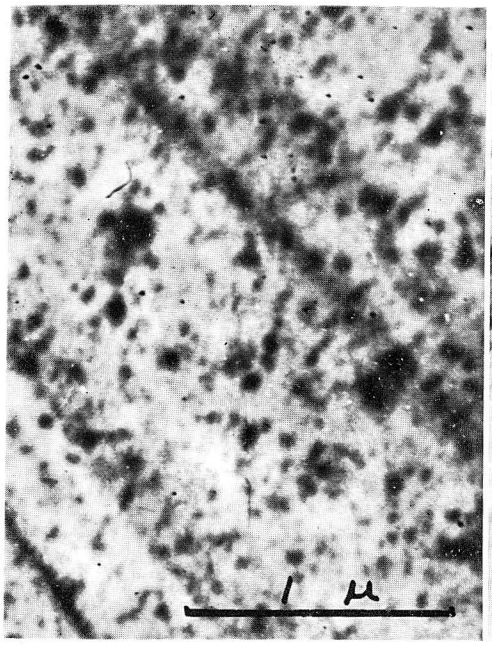

Photo. 23 Al-4% Cu alloy, W.Q., aged for 4 days at 110°C. ×35000

Photo. 24 Al-4% Cu alloy, W.Q., 5.0% elong., aged for 4 days at 110°C. ×35000

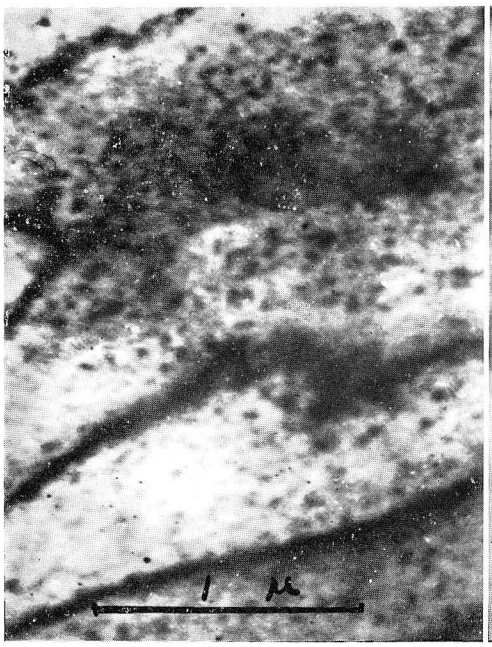

Photo. 25 Al-4% Cu alloy, W.Q., 40% rolled, aged for 4 days at 110°C. ×35000

Photo. 26 Al-4% Cu alloy, W.Q., aged for 6 days at 160°C. ×27000

Photo. 27 Al-4% Cu alloy, W. Q., 5.0% elong., aged for 6 days at 160°C. ×54000

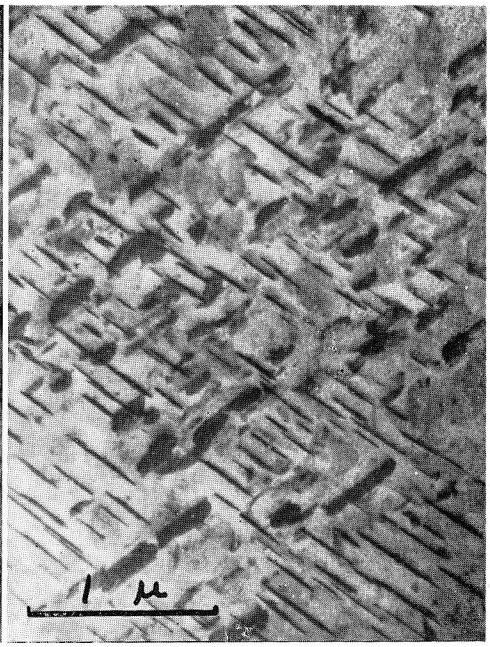

Photo. 28 Al-4% Cu alloy, W.Q., aged for 1 day at 200°C. ×25000

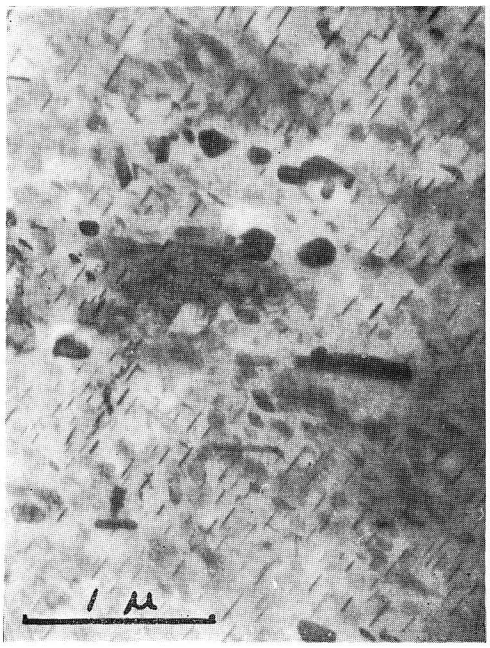

Photo. 29 Al-4% Cu alloy, W.Q., 40% rolled, aged for 1 day at 200°C. ×25000

Photo. 30 Al-4% Cu alloy, W.Q., 70% rolled, aged for 1 day at 200°C. ×25000

Photo. 31 Al-Cu-Zr alloy, W.Q., aged for 70 days at 70°C. ×30000

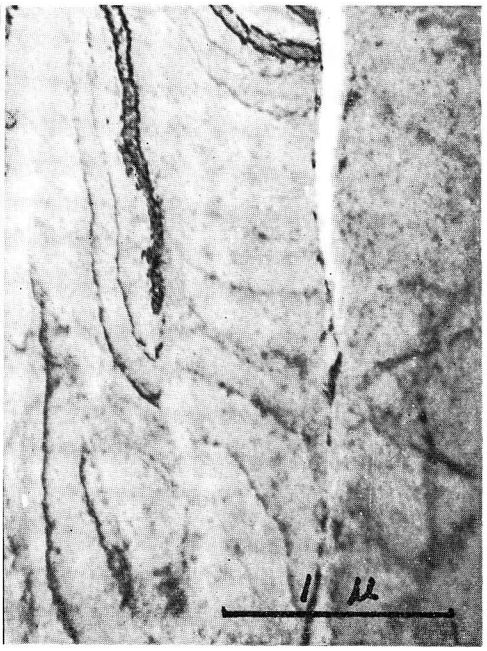

Photo. 32 Al-Cu-Zr alloy, W.Q., 70% rolled, aged for 70 days at 70°C. ×30000

Photo. 33 Al-Cu-Zr alloy, W.Q., aged for 1 day at 150°C. ×25000

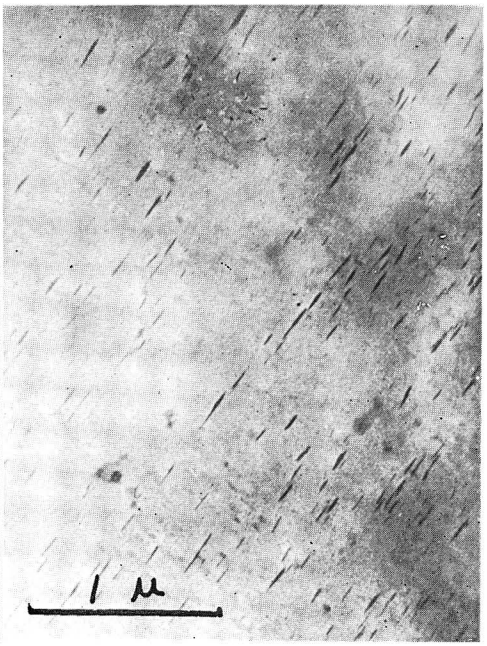

Photo. 34 Al-Cu-Zr alloy, W.Q., 5.0% elong., aged for 1 day at 150°C. ×25000

Photo. 35 Al-Cu-0.3% Be alloy, W.Q., 5.0% elong., aged for 1 day at 200°C. ×25000

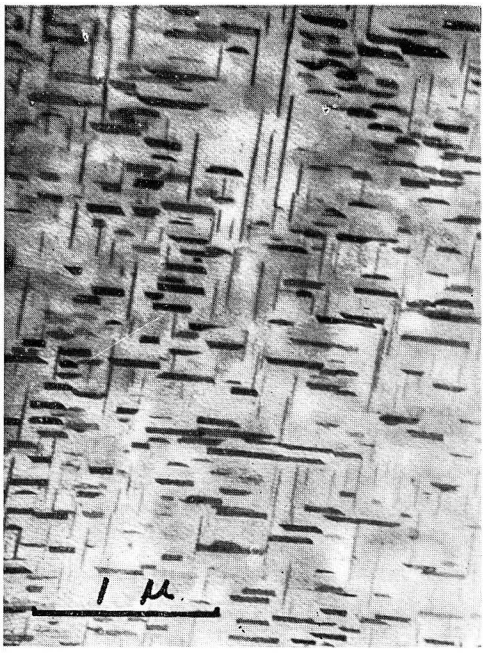

Photo. 36 Al-Cu-Ti alloy, W.Q., aged for 1 day at 200°C. ×25000

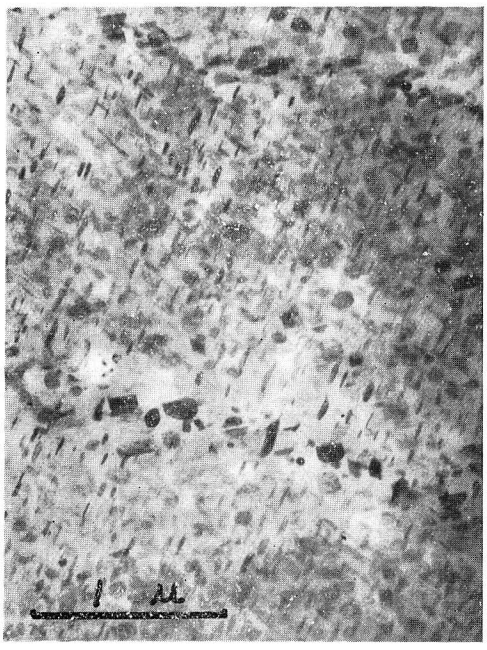

Photo. 37 Al-Cu-Ti alloy, W.Q., 40% rolled, aged for 1 day at 200°C. ×25000

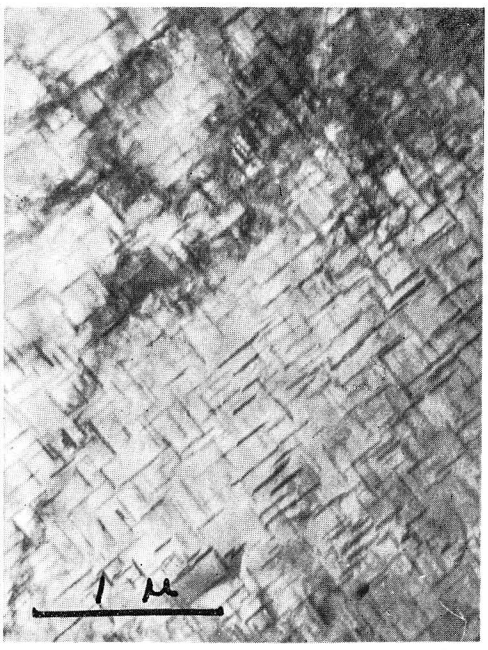

Photo. 38 Al-Cu-Zr alloy, W.Q., aged for 1 day at 200°C. ×25000

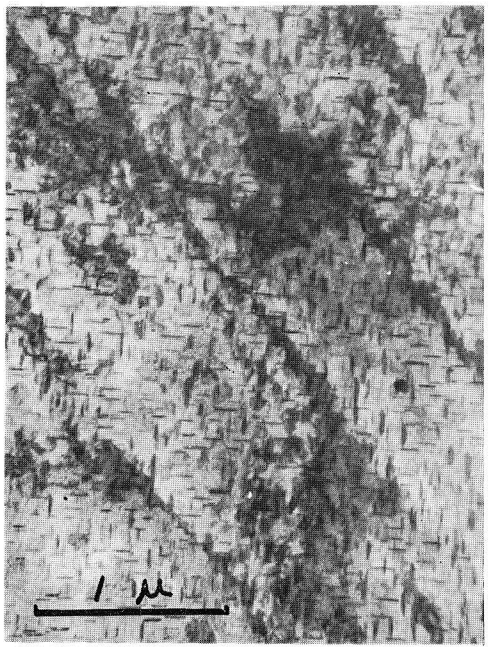

Photo. 39 Al-Cu-Zr alloy, W.Q., 40% rolled, aged for 1 day at 200°C. ×25000

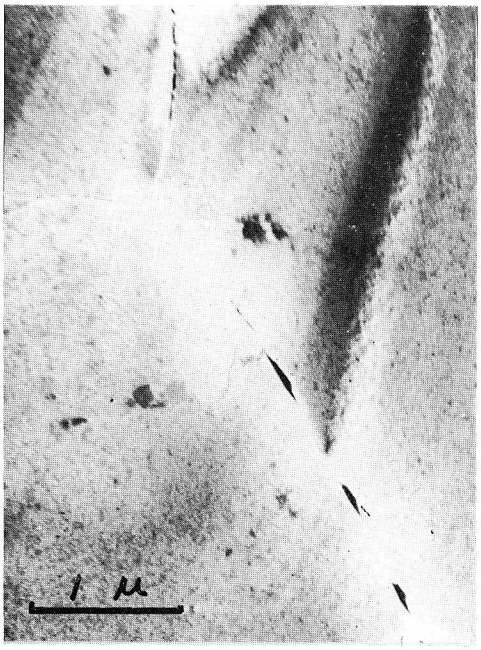

Photo. 40 Al-20% Ag alloy, W.Q., aged for 14 days at 70°C. ×20000

Photo. 41 Al-20% Ag alloy, W.Q., aged for 1 day at 110°C. ×20000

Photo. 42 Al-20% Ag alloy, W.Q., aged for 4 days at 110°C. ×20000

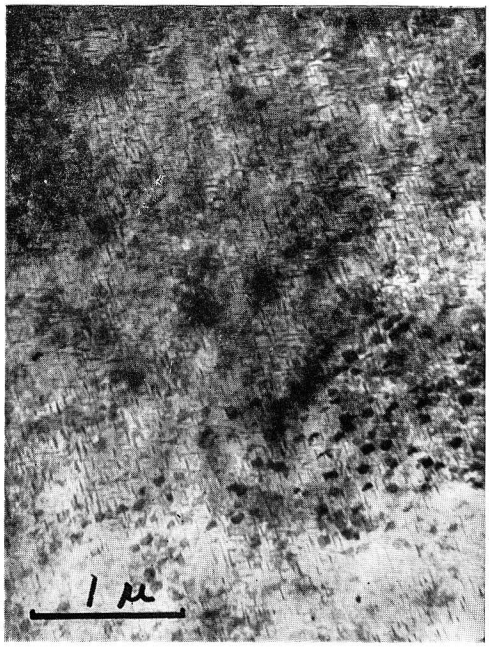

Photo. 43 Al–20% Ag alloy, W.Q., 20% rolled, aged for 4 days at 110°C. ×20000

Photo. 44 Al–Ag–Zr alloy, W.Q., aged for 1 day at 110°C. ×20000

Photo. 45 Al–Ag–Zr alloy, W.Q., aged for 4 days at 110°C. ×20000

Photo. 46 Al–Ag–Zr alloy, W.Q., aged for 4 days at 110°C. ×20000

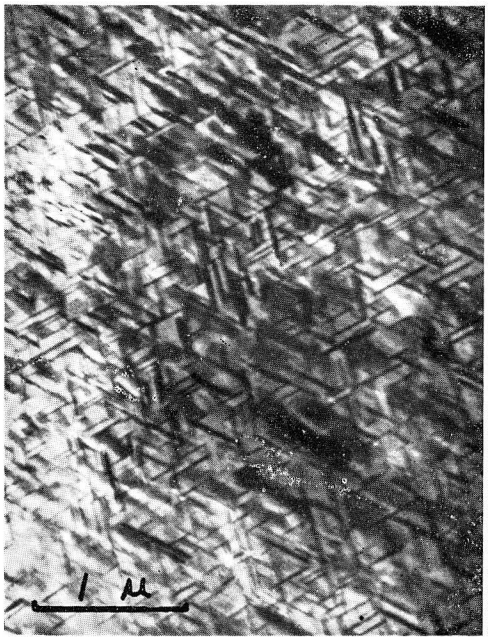

Photo. 47 Al-Ag-Zr alloy, W.Q., 20% rolled, aged for 4 days at 110°C. ×20000

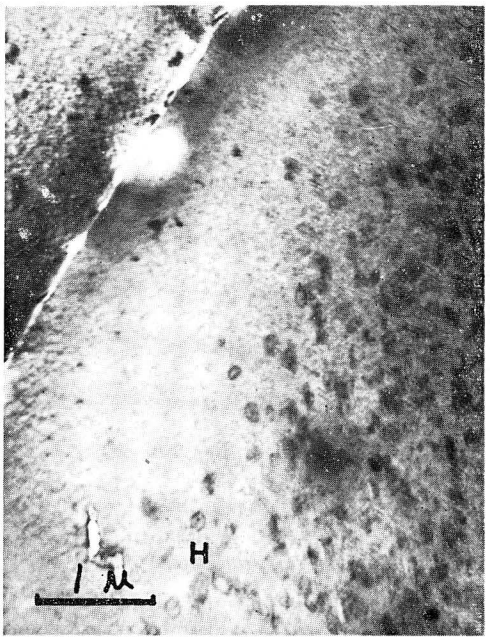

Photo. 48 Al-20% Ag alloy, W.Q., aged for 0.5 hrs at 200°C. ×15000

Photo. 49 Al-20% Ag alloy, W.Q., aged for 4 hrs at 200°C. ×20000

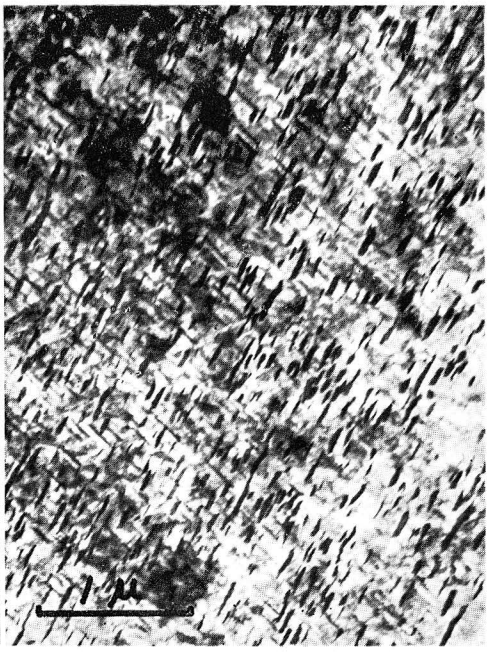

Photo. 50 Al-20% Ag alloy, W.Q., 20% rolled, aged for 4 hrs at 200°C, ×20000

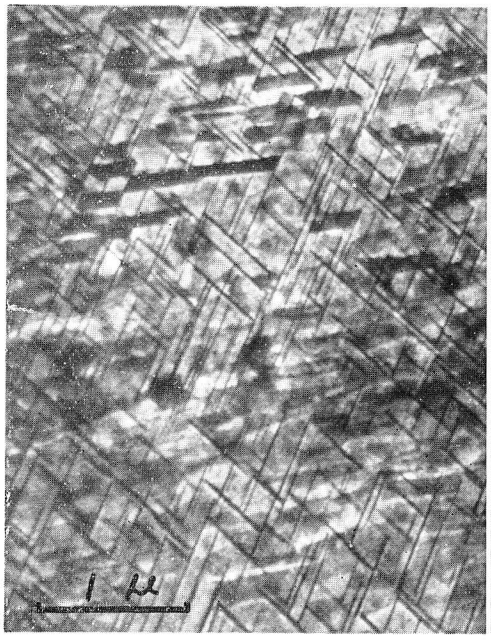

Photo. 51 Al–Ag–Zr alloy, W.Q., aged for 4 hrs at 200°C. ×20000

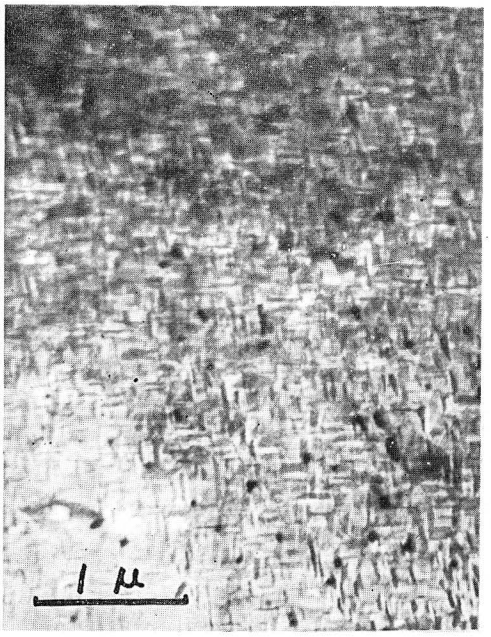

Photo. 52 Al–Ag–Zr alloy, W.Q., 20% rolled, aged for 4 hrs at 200°C. ×20000